Available online at www.sciencedirect.com
ScienceDirect
Atmospheric Environment 41 (2007) 2683–2698
ATMOSPHERIC ENVIRONMENT
www.elsevier.com/locate/atmosenv

Review

A review of parameterizations for modelling dry deposition and scavenging of radionuclides

Bruno Sportisse*

Research Center in Atmospheric Environment (CEREA), Joint Laboratory Ecole Nationale des Ponts et Chaussées/ Electricité de France R&D, 6-8 Avenue Blaise Pascal, 77455 Champs sur Marne, France

Received 26 July 2006; received in revised form 16 November 2006; accepted 23 November 2006

Abstract

This article aims at reviewing the state-of-the-science parameterizations for modelling dry deposition and scavenging of atmospheric tracers, with a focus on radionuclides. These parameterizations are key components of the numerical models that are used for environmental forecast. We present detailed models and parameterizations. Both are characterized by many uncertainties.

Keywords: Dispersion models; Dry deposition; Wet scavenging; Parameterizations

Contents

*Tel.: +33 1 64 15 21 41; fax: +33 1 64 15 21 70.
E-mail address: bruno.sportisse@cerea.enpc.fr.

1352-2310/$ - see front matter
doi:10.1016/j.atmosenv.2006.11.057

0. Introduction

Dry deposition and scavenging processes (rainout and washout) are key processes for the evolution of radionuclides in the atmosphere. The current state-of-the-science dispersion models (the so-called chemistry-transport models) used for radionuclides strongly rely on parameterizations for these processes.

There are however many sources of uncertainty. The first source is related to the meteorological fields, especially the rain intensity or the cloud characteristics (liquid water content and diagnosis) for scavenging. The second source is related to the microphysical description of the processes. The behaviour of radionuclides is strongly related to their chemical form as they may be released in the atmosphere as gases and particles. For instance, it is usually assumed that most of cesium is bound to particles (aerosols) while iodine is either bound to atmospheric aerosols or in gaseous form (elemental form and organic iodine CH_3I). The partitioning between gaseous form and particles and the size distribution of aerosols strongly affect dry deposition and scavenging.

Wet scavenging is usually parameterized by $\mathrm{d}c/\mathrm{d}t = -\Lambda c$ with c the concentration and Λ the scavenging coefficient (in s^{-1}). One usually distinguishes in-cloud scavenging (*rainout*) and below-cloud scavenging by raindrops (*washout*). It is often recognized that the wet scavenging of radionuclides is mainly related to particles (Chamberlain, 1991, p. 133) and is more important for rainout. The parameterizations are highly uncertain due to the difficulty of characterizing the aerosol distribution and the uncertainties for rain intensity.

Dry deposition is often applied as a boundary condition for vertical turbulent diffusion through $K_z \nabla c \cdot \mathbf{n} = E - v_{\mathrm{dep}} c$ with K_z the eddy coefficient, E the surface emission (possibly for resuspension) and v_{dep} the dry deposition velocity. $\mathbf{n}$ is the unit vector oriented upwards. The deposition velocity depends on the surface meteorological fields, on the land use coverage and on the physical and chemical properties of the tracer.

Parameterization for Λ and v_{dep} are therefore required for 3D modelling. Many articles have already been devoted to these topics, ranging from theoretical studies focussed on detailed modelling to empirical parameterizations. The objective of this paper is to summarize the available parameterizations (to our knowledge), to underline the common characteristics and the differences and to investigate the uncertainties. The hope is that it may be useful for a modeller to have the synthesis of the majority of published data.

This article is structured as follows. We briefly summarize in Section 1 the key facts for the possible form of the radionuclides in the atmosphere. We emphasize on the measurements following the Chernobyl accident. Detailed and parameterized models are given in Sections 2 and 3 for dry deposition and wet scavenging, respectively. For each process, detailed models are presented and then empirical models, usually based on tuning to measurements. The focus is put on particles and wet scavenging. The article ends with conclusions.

1. Background for radionuclides

Three features have a strong impact for the loss properties of atmospheric radionuclides: the partitioning between gases and aerosols, the partitioning between the organic and inorganic forms and the aerosol size distribution.

Gas/aerosol partitioning: The radionuclides may be released into the atmosphere as gases and/or particles. The partitioning between both phases is a crucial issue for loss processes and there are many uncertainties reported in the literature, especially following the Chernobyl accident. For instance, short-range measurements (Ogorodnikov et al., 1994) indicate a gaseous fraction ranging from 30% to 90% of the total mass. Measurements in Great Britain (Clark and Smith, 1988) give a ratio of particle mass to gaseous mass ranging from $\frac{1}{3}$ to $\frac{1}{2}$. This ratio is estimated to range from $\frac{1}{5}$ to $\frac{1}{3}$ in Germany (München, Chamberlain, 1991, p. 124), to be of magnitude $\frac{1}{4}$ in Sweden (Chamberlain, 1991, p. 84) and to vary with time. Baklanov and Sorensen (2001) estimate that 70% of the total release was in gaseous form during the first weeks (up to 90% of iodine emissions; see also Pöllänen et al., 1997). Other measurements indicate a gaseous fraction ranging from 50% to 85% in southern Finland (Jylhä, 1991).

Some theoretical studies have tried to compute the partitioning between both phases. For instance, in Budyka (2000), a condensation/evaporation model (unfortunately poorly detailed) gives the evolution of mass transfer between the gaseous and the particulate phases. The resulting gaseous fraction depends on the total atmospheric aerosol concentrations (10, 30, $100\,\mu g\,m^{-3}$, standard values over Europe) and the size distribution (the diameters are in the range 0.015–0.4 μm). The resulting aerosol is centred around 0.5 μm with a gaseous fraction of 15% (for a total atmospheric aerosol concentration of $100\,\mu g\,m^{-3}$), 35% (for $30\,\mu g\,m^{-3}$) and 60% (for $10\,\mu g\,m^{-3}$).

Organic/inorganic partitioning: Another source of uncertainties is related to the inorganic/organic partitioning for iodine. The dissolution properties are indeed not similar. For instance, the measurements in München (cited above) indicate a growth of the organic part (from 43% to 59% of the total mass, including gas and aerosols) due to the atmospheric ageing.

Aerosol size distribution: Besides the chemical composition, the loss processes strongly depend on the aerosol size distribution, through nonlinear processes (see the next sections). Hereafter, r_p will stand for the particle radius, d_p for the particle diameter.

For the Chernobyl accident, most authors reported that the aerosols were in the submicronic range ($r_p < 1$ or 2 μm in Brandt et al., 2002; Chamberlain, 1991, pp. 86 and 92). In Ogorodnikov et al. (1994), the size of the emitted particles differ according to the period.

In the first weeks, emissions are in the submicronic range (with an aerosol mean aerodynamic diameter (AMAD) or d_a, of 0.6–0.7 μm). We recall that for a particle density $\rho_p \simeq 1.4\,g\,cm^{-3}$, $d_a \simeq 1.2 \times d_p$. This is in coherence with data from Baklanov and Sorensen (2001). Some typical values of particle distributions can be found for iodine and cesium in Table 1 (Baklanov and Sorensen, 2001). The aerosol distribution is a lognormal law of variance σ, centred around the AMAD. Jylhä (1991) reports a size distribution of $[0.65-0.93]$ μm for cesium 137 and of $[0.33-0.57]$ μm for particulate iodine. This reference also indicates that rain measurements in Switzerland illustrate the bounds to "classical aerosols" (sulfates/nitrates). Sparmacher et al. (1993) report a measured aerosol distribution (in Germany) from 10 nm to 5 μm, centred around 1 μm.

Table 1
Particle distribution of cesium and iodine (Baklanov and Sorensen, 2001, following the Chernobyl accident)

Radionuclide	v_{dep} ($cm\,s^{-1}$)	AMAD (μm)	σ
^{137}Cs	0.1	0.68	1.8–2.5
^{134}Cs	0.12	0.59	2–2.5
^{131}I	0.6	0.48	3–4
^{133}I	0.7	0.6	—

In the second period (after the building of the sarcophage), the AMAD was up to 6–7 μm due to resuspension. Moreover, many studies (for instance Pöllänen et al., 1997) report coarse radioactive particles ("hot spots" beyond 20 μm) measured in Northern and Eastern Europe.

2. Dry deposition

2.1. Field measurement data

There are many references devoted to measurement data of dry deposition. For radionuclides, we focus here on particles. All the measured data indicate the sensitivity to the size distribution. Garland (2001) reviews some methods that are currently used (typically throughfall and eddy correlation methods). The measurements are usually characterized by a large uncertainty (Fig. 1). We refer to the discussion in Garland (2001) and to the review in Gallagher et al. (1999).

Garland (2001) reported a "mean" value $v_{dep} = 0.5\,cm\,s^{-1}$ for cesium, derived from measurements following the Chernobyl accident. However, the value strongly depends on the natural surface: $0.05\,cm\,s^{-1}$ for grass, $[0.07-0.55]\,cm\,s^{-1}$ for forest (the weakest value is for conifers). These values are coherent with those used in models with constant deposition velocities (see below). Notice that these constant values do not describe the strong sensitivity with respect to the size distribution (Fig. 1).

2.2. Detailed models

2.2.1. For gases

Key references are Wesely (1989) and Wesely and Hicks (2000). The deposition process is usually

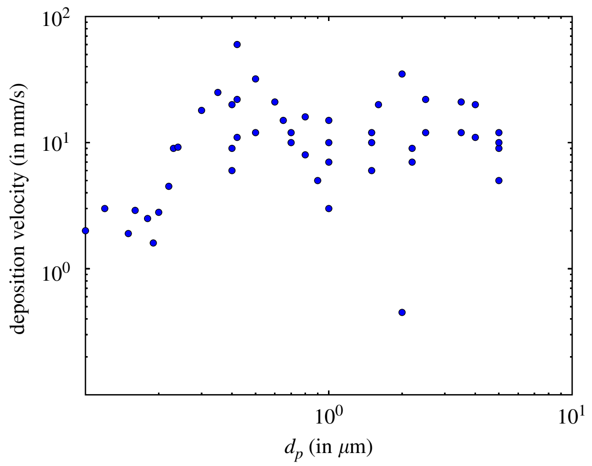

Fig. 1. Measured deposition of particles to forest (adapted from Gallagher et al., 1999).

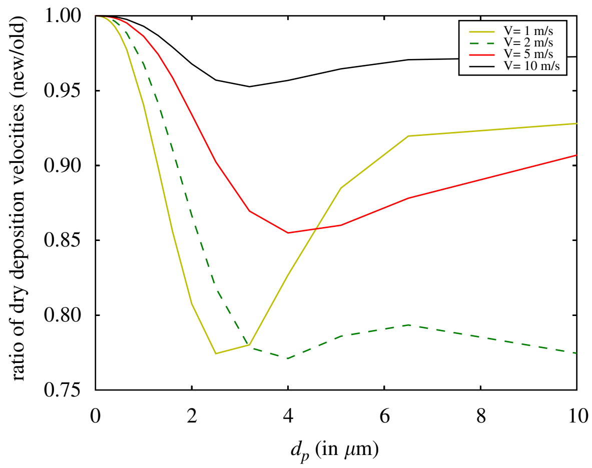

Fig. 2. Distribution of the ratio of dry deposition velocities (the new parameterization corresponds to Venkatram and Pleim (1999), the old parameterization to the classical formula) with respect to the aerosol diameter, for different values of wind velocity. The particle density is $\rho_p = 1\,\mathrm{g\,cm^{-3}}$. The land use coverage is "needleleaf trees" in summer.

interpreted in analogy to electrical resistance. The deposition to the surface is supposed to be controlled by three resistances in series: the aerodynamic resistance (R_a), the quasi-laminar layer resistance (R_b) and the surface resistance (R_s). The total resistance (the inverse of the dry deposition velocity) is defined by the sum of these three resistances

$$v_{dep} = \frac{1}{R_a + R_b + R_s}. \tag{1}$$

The possible expression of the resistances can be found in classical textbooks (for instance Seinfeld and Pandis, 1998). For the sake of clarity, we do not enter into details.

2.2.2. For particles

For particles, the particle settling is supposed to operate in parallel with the previous processes. Moreover, one usually assumes that the surface resistance can be neglected because the particles adhere to the surface. With the electric resistance analogy, one gets (Seinfeld and Pandis, 1998):

$$v_{dep} = u_{grav} + \frac{1}{R_a + R_b + R_a R_b u_{grav}}, \tag{2}$$

where u_{grav} is the gravitational settling velocity (see below for the computation).

An alternative formula for the dry deposition velocity is (Venkatram and Pleim, 1999)

$$v_{dep} = \frac{u_{grav}}{1 - e^{-(R_a+R_b)u_{grav}}}. \tag{3}$$

The advantage of this parameterization is that it satisfies mass conservation.

The ratio of the dry deposition velocity computed with Eq. (3) to this computed with Eq. (2) is given in Fig. 2 for aerosols of density $1\,\mathrm{g\,cm^{-3}}$. The ratio is computed for different wind velocities as a function of the aerosol diameter. The computation of the resistances follows Zhang et al. (2001) and takes into account Brownian diffusion, inertial deposition and interception by ground.

Eq. (3) leads to smaller values of v_{dep} (the reduction is up to 20% for the largest particles for low wind velocities). Notice that the differences may be significant (as opposed to what is surprisingly reported in Venkatram and Pleim, 1999).

The parameterization of the dry deposition to water surface may also follow different laws. We refer for instance to Pryor et al. (1999) and Travnikov and Ilyin (2005).

Gravitational settling velocity: For small particles, say $d_p \leqslant 20\,\mu\mathrm{m}$, u_{grav} is given by the Stokes formula (for instance Seinfeld and Pandis, 1998)

$$u_{grav} = \frac{d_p^2(\rho_p - \rho_{air}) g C_c}{18\mu_{air}}, \tag{4}$$

where ρ_p (in $\mathrm{kg\,m^{-3}}$) is the particle density, μ_{air} the dynamic viscosity of air (in Pa s) and g the gravity constant (in $\mathrm{m\,s^{-2}}$). C_c is the Cunningham correction factor that takes into account the slipping effects for the finest particles:

$$C_c = 1 + \frac{2\lambda_{air}}{d_p}\left(1.257 + 0.4\exp\left(-0.55\frac{d_p}{\lambda_{air}}\right)\right), \quad (5)$$

where λ_{air} is the air mean free path (in m): $\lambda_{air} = 2\mu_{air}/(P\sqrt{8/\pi RT})$, with R the gas constant (in $J\,K^{-1}\,kg^{-1}$), T the temperature (in K) and P the pressure (in Pa).

For larger particles (or cloud droplets), the Stokes law in no longer valid and one needs to use a drag coefficient. A nonlinear system has to be solved (Seinfeld and Pandis, 1998):

$$u_{grav} = \sqrt{\frac{4gd_pC_c\rho_p}{3C_D\rho_{air}}}, \quad (6)$$

where the drag coefficient C_D is an analytical function of the Reynolds number of the particle (and, as such, a function of u_{grav}). This equation can be solved by a Newton algorithm in few iterations. One also refers to Näslund and Thaning (1991). Notice that there exit many available parameterizations for the drag coefficient. The parameterization given in Näslund and Thaning (1991) has the advantage of providing a smooth function (as opposed to this of Seinfeld and Pandis, 1998).

2.3. Parameterized models

Some reference values for the dry deposition of iodine and cesium can be found in Table 2 (following Brandt et al., 2002). Additionally, the maximal values of dry deposition velocities are provided as a function of the land use coverage in Table 3.

It is sometimes advocated to relate the dry deposition velocities of radionuclides to the corresponding form of SO_x, that is to say to use SO_2 as a typical gas-phase component and sulfate aerosols (SO_4^{2-}) as a typical particle. For instance, for the EURAD model (Haas et al., 1990), the dry deposition velocity of cesium is half of this of aerosol sulfate. Baklanov and Sorensen (2001) reports the use of the dry deposition velocity of SO_2 for gas-phase iodine ($0.5\,cm\,s^{-1}$ for Baklanov and Sorensen, 2001) and the one of sulfate aerosols for particulate iodine ($0.1\,cm\,s^{-1}$).

In Baklanov (1999, p. 11), $0.05\,cm\,s^{-1}$ is the reference value for cesium 137. In Brandt et al. (2002), the default value for all species is $0.2\,cm\,s^{-1}$. In Raes et al. (1991), the reference is the dry deposition of accumulation mode of aerosols, $0.1\,cm\,s^{-1}$. For the modelling system RODOS (Päsler-Sauer, 2003, p. 16), some typical values are given for dry deposition over lawn with a wind at 10 m above the ground of $4\,m\,s^{-1}$: $0.8\,cm\,s^{-1}$ for elemental iodine, $0.01\,cm\,s^{-1}$ for organic iodine and $0.1\,cm\,s^{-1}$ for aerosols. The RIMPUFF model (a component of RODOS, Thykier-Nielsen et al., 1999, pp. 20–23) indicates values of $1\,cm\,s^{-1}$ for elemental iodine, $0.05\,cm\,s^{-1}$ for organic iodine and 0.1 for aerosols. These values are summarized in Table 3.

Table 2
Some values of dry deposition velocities (in $cm\,s^{-1}$) from literature (from Brandt et al., 2002)

Reference	^{131}I	^{137}Cs
Hanna et al. (1991)	0.3	0.1
Maryon et al. (1992)	0.5	0.05
Klug et al. (1992)	0.15–2.0	0.1–0.5
Slinn and Slinne (1980)	—	0.31
Sehmel (1980)	0.1–2.0	0.04–0.5

Table 3
Values of dry deposition velocities (in $cm\,s^{-1}$) (from Müller and Pröhl, 1993; Baklanov and Sorensen, 2001) according to the land use coverage (LUC) and for the RODOS system (Päsler-Sauer, 2003; Thykier-Nielsen et al., 1999)

LUC	Particulate	Elemental iodine	Organic iodine
Soil	0.05	0.3	0.005
Grass	1.05	0.15	0.015
Trees	0.5	5	0.05
Other plants	0.2	2	0.02
RODOS	0.1	0.8	0.01
RIMPUFF	0.1	1	0.05

We also refer to Garland (2001) for a discussion of the gap between model results and observational data. A possible explanation is that the models may omit electrical effects and thermo- and diffusion-phoretic forces.

In Quélo et al. (2006), we have used a robust approach by taking $0.2\,cm\,s^{-1}$ for iodine and 0.2 or $0.1\,cm\,s^{-1}$ for cesium (with model-to-data comparisons for the Chernobyl and Algeciras cases).

A common feature of these parameterizations is that the dry deposition velocity of elemental iodine is greater than the one of aerosols, which is greater than the one of organic iodine.

3. Wet scavenging

Wet scavenging is usually partitioned in *in-cloud* scavenging and *below-cloud* scavenging. Some authors advocate rather to distinguish *nucleation scavenging* and *impaction scavenging* in order to give a more accurate process description (see the discussion in Tost et al., 2006). Even if rainout is a key process, we focus on below-cloud scavenging because there are not a lot of data related to in-cloud scavenging.

3.1. Field measurement data

The experimental data indicate a strong sensitivity of the scavenging coefficient with respect to the particle size. The scavenging is much stronger for particles below, let say, 0.3 μm or above 1–2 μm than for particles in the so-called Greenfield gap (typically in the range [0.3−1] μm, Greenfield, 1957). The measured data are highly "scattered" (Fig. 3 as an example) and the model-to-data comparison is usually difficult to perform.

Many data are the basis of the fitting presented in Section 3.3 (for instance Sparmacher et al., 1993).

3.2. Detailed models

A crucial issue is to fix the distribution of the raindrops and the resulting falling velocities. We first describe models of rain and then the scavenging of gases and particles.

3.2.1. Representation of the rain

In the following, p_0 is the rain intensity (in $\mathrm{mm\,h^{-1}}$). D_r (in meter) stands either for the raindrop diameter of a monodisperse distribution or for the representative diameter of a polydisperse distribution. Other units are always mentioned.

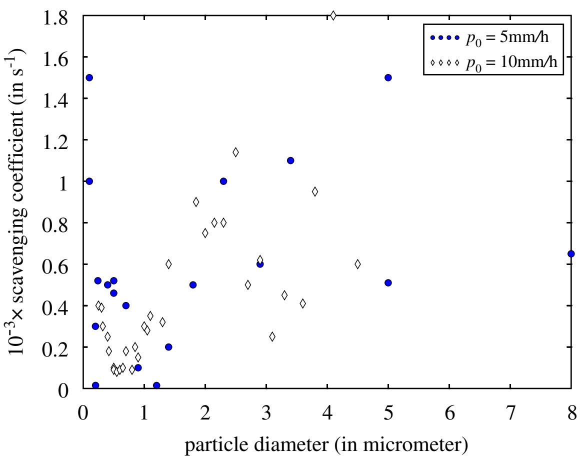

Fig. 3. Measured scavenging coefficient for two rain intensities ($p_0 = 5$ and $10\,\mathrm{mm\,h^{-1}}$), from Baklanov and Sorensen (2001) and the references therein. These values are given as illustration for the "scattering".

3.2.1.1. Raindrop distribution. The raindrop distribution is usually described by a Gamma function with four parameters

$$n_\mathrm{r}(D_\mathrm{r}) = \alpha_0 D_\mathrm{r}^{\alpha} \exp(-\beta D_\mathrm{r}^{\gamma}). \quad (7)$$

The two classical cases are the Marshall–Palmer distribution ($\alpha = 0$; $\gamma = 1$) and the Khrigian–Mazin distribution ($\alpha = 2$, $\gamma = 1$). We refer to Table 4. It is usually recognized that the Marshall–Palmer distribution leads to an overestimation of the finest droplets.

de Wolf (2001) proposes a distribution based on a fit to measurements as a function of the rain intensity

$$n_\mathrm{r}(D_\mathrm{r}) = \alpha(p_0) \times 2.6 \times 10^{-6} p_0^{-0.384} D_\mathrm{r}^{2.93} \times \exp(-2.69 p_0^{-0.186} D_\mathrm{r}), \quad (8)$$

with the normalization factor $\alpha(p_0) = 1.047 - 0.0436\ \ln p_0 + 7.34 \times 10^{-3} (\ln p_0)^2$. We refer to the discussion in Henzing et al. (2006) for a comparison of the different parameterizations and the impact for below-cloud scavenging of particles.

In Mircea et al. (2000), lognormal distributions are proposed on the basis of measurements.

3.2.1.2. Representative diameter. There exist several parameterizations for the representative diameter of raindrops of the form $D_\mathrm{r} = A p_0^B$ (see Table 5, in mm there):

$$D_\mathrm{r} = [0.2431 - 0.97] p_0^{[0.158-0.25]}. \quad (9)$$

The comparison between the parameterizations is given in Fig. 4. One notices the spread of results, especially for large rain intensities. As already said, the Marshall–Palmer distribution leads to an over-

Table 4
Typical ranges for raindrop diameters given by the Marshall–Palmer and Khrigian–Mazin distributions (Mircea and Stefan, 1998)

Rain type	p_0 ($\mathrm{mm\,h^{-1}}$)	Range for D_r (mm)
Weak	[1–5]	[0/0.001–0.1]
Moderate	[5–100]	[0/0.01–1]
Strong	[100–500]	[0/0.1–10]

In the notation $[a/b-.]$, a stands for the lower value of the Marshall–Palmer distribution, b for the one of the Khrigian–Mazin distribution.

estimation of finest droplets (which results in the overestimation of collision efficiencies and then of scavenging; see below).

Table 5
Some parameterizations for the representative diameter of raindrops, D_r (here in mm)

Index	Reference	D_r (mm)
1	Pruppacher and Klett (1998, p. 34)	$0.976 \times p_0^{0.21}$
2	Marshall–Palmer	$0.243\,p_0^{0.21}$
3	Andronache (2004)	$0.24364\,p_0^{0.214}$
4	Loosmore and Cederwall (2004)	$0.97\,p_0^{0.158}$
5	Mircea et al. (2000)	$[0.63-0.72]p_0^{0.23}$
6	Underwood (2001, p. 35)	$0.7p_0^{0.25}$

Mircea et al. (2000) uses measurements over the Eastern Mediterranean area (which results in a range and not in a given value).

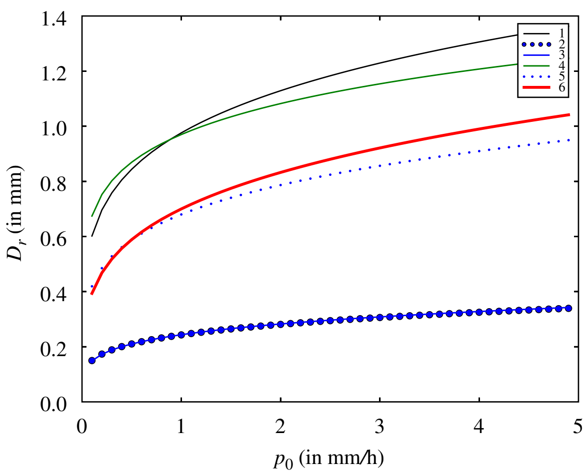

Fig. 4. Evolution of the representative diameter as a function of the rain intensity for different parameterizations. The index is given in Table 5.

3.2.1.3. Falling velocity. The falling velocity U_{drop} (in $\mathrm{m\,s^{-1}}$) can be computed as a function of diameters through different parameterizations (Table 6). For the terminal velocity, due to the size of falling raindrops (of diameter bigger than 20 μm), the Stokes formula (4) cannot be used and a system similar to (6) has to be used

$$U_{\text{drop}} = \sqrt{\frac{4gD_r C_c \rho_{\text{water}}}{3C_D \rho_{\text{air}}}} \qquad (10)$$

Comparisons among the parameterizations are given in Fig. 5 with the parameterization "4" of the representative diameter (index = 4 of Table 5). The discontinuity for the index 3 is related to the change of the computation of the drag coefficient for particle Reynolds number greater than 500.

3.2.2. Scavenging of gases

Notice that these detailed models are already parameterized versions of microphysical models (see for instance Sportisse and Du Bois, 2002; Sportisse and Djouad, 2003 for the justifications).

3.2.2.1. Below-cloud scavenging (washout). We refer for instance to Sportisse and Du Bois (2002). The scavenging coefficient for a gas is given by

$$\Lambda = \frac{6LD_g Sh}{D_r^2} \exp\left(\frac{6D_g Sh\, z}{D_r^2 U_{\text{drop}} HRT}\right), \qquad (11)$$

with L the liquid water content for rain (volume of falling water per volume of air), D_g the molecular gas-phase diffusivity for the scavenged gas, H the Henry's coefficient (the efficient coefficient if the acidity of the rain is taken into account). Sh is the Sherwood number:

$$Sh = 2 + 0.6\left(\frac{U_{\text{drop}} D_r}{\nu_{\text{air}}}\right)^{1/2}\left(\frac{\nu_{\text{air}}}{D_g}\right)^{1/3}, \qquad (12)$$

Table 6
Some parameterizations for the falling velocity of raindrops (in $\mathrm{m\,s^{-1}}$)

Index	Reference	U_{drop} ($\mathrm{m\,s^{-1}}$)
1	Kessler (Andronache, 2003, p. 143; Mircea and Stefan, 1998, Table 2)	$130\sqrt{D_r}$
2	Seinfeld (1985, p. 632)	$9.58\left[1-\exp\left(-\left(\frac{D_r}{0.171\times10^{-2}}\right)^{1.147}\right)\right]$
3	Seinfeld and Pandis (1998) and Mircea et al. (2000)	Terminal velocity
4	Andronache (2004)	$3.778 \times 10^3 D_r^{0.67}$
5	Loosmore and Cederwall (2004)	$4.854\,D_r \exp(-195 \times 10^{-3} D_r)$

D_r is in meter.

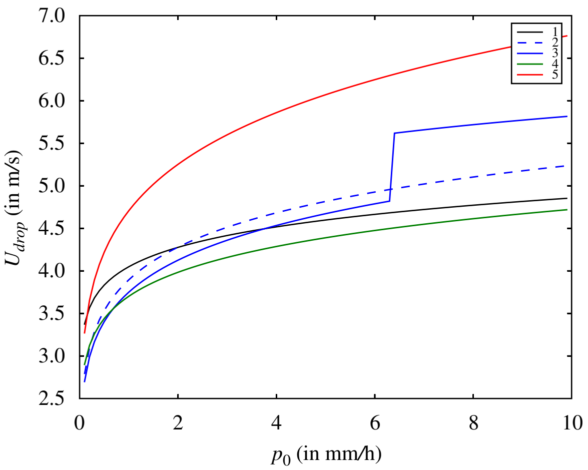

Fig. 5. Evolution of the falling velocity of raindrops with respect to rain intensity. The index is related to the parameterization of falling velocity. The representative diameter is computed with the parameterization "4" for D_r.

with $\nu_{air} = \mu_{air}/\rho_{air}$ the kinematic viscosity of air (in $m^2\,s^{-1}$). z is the distance of the falling raindrop from the cloud.

3.2.2.2. In-cloud scavenging (rainout). In-cloud scavenging is much more difficult to parameterize especially because aqueous-phase chemistry has to be taken into account. We refer for instance to Sportisse and Djouad (2003) for a rigorous derivation of kinetic mass transfer coefficients. We also refer to Tost et al. (2006) for the description of a detailed coupled model between the gas phase and the aqueous phase.

A simplified model is given in Roselle and Binkowski (1999)

$$\Lambda = -\frac{1 - e^{-\tau_{cld}/\tau_{washout}}}{\tau_{cld}}, \tag{13}$$

where τ_{cld} (in second) is the 3D timestep of the dispersion model if the cloud size exceeds the cell dimension, and is equal to 1 h otherwise. $\tau_{washout}$ is the time required for the volume of water to precipitate to the ground. For a cloud of liquid water content L (in volume per volume), of depth Δz_{cld} and of total (air) volume V, $\tau_{washout}$ depends on the precipitation rate p_0 (in $m\,s^{-1}$) through $LV = \tau_{washout} p_0 S$, where S is the ground surface covered by the cloud. If we assume that $V = S\Delta z_{cld}$, one gets $\tau_{washout} = L\Delta z_{cld}/p_0$.

3.2.3. Scavenging of particles

The aerosol radius and diameter for a monodisperse distribution are r_p and d_p (in μm), respectively. In the following, we focus on the *washout* of particles (*below-cloud scavenging*), which corresponds to the scavenging for falling raindrops.

3.2.3.1. Scavenging coefficient for a monodisperse distribution. The scavenging rate of particles of diameter d_p is given by

$$\frac{dn_p(d_p)}{dt} = -\Lambda(d_p) n_p(d_p). \tag{14}$$

The scavenging coefficient $\Lambda(d_p)$ is computed on the basis of the number of particles collected per time unit by raindrops. For a monodisperse distribution of raindrops, of representative diameter D_r, this gives

$$\Lambda(d_p) = \frac{\pi}{4} D_r^2 U_{drop}(D_r) E(D_r, d_p) N_r, \tag{15}$$

with $E(D_r, d_p)$ the collision efficiency and N_r the total density of raindrops (in m^{-3}). The collision efficiency is defined as the fraction of the particles of diameter d_p in the collision volume of the raindrop of diameter D_r that are actually scavenged. This formula assumes that the raindrop falling velocity is much bigger than the settling velocity of aerosols and that the representative diameter for raindrops is also much bigger than the aerosol diameter, which is met in practice.

As the rain intensity p_0 (here in $m\,s^{-1}$) is defined by

$$p_0 = \int_0^\infty \frac{\pi}{6} D_r^3 U_{drop}(D_r) n_r(D_r)\, dD_r \tag{16}$$

one gets in the monodisperse case $p_0 = (\pi/6) D_r^3 U_{drop}(D_r) N_r$. The scavenging coefficient is therefore

$$\Lambda(d_p) = \frac{3}{2} \frac{E(D_r, d_p) p_0}{D_r}. \tag{17}$$

3.2.3.2. Scavenging coefficient for a polydisperse distribution. Let us consider a polydisperse distribution for raindrops, given by $n_r(D_r)$ (in $m^{-3}\,m^{-1}$). The scavenging coefficient is then integrated over the raindrop distribution

$$\Lambda(d_p) = \int_0^\infty \frac{\pi}{4} D_r^2 U_{drop}(D_r) E(D_r, d_p) n_r(D_r)\, dD_r. \tag{18}$$

A special attention has to be paid to the numerical integration due to the vanishing part of the distribution (tests not reported here).

3.2.3.3. Collision efficiency. A crucial point is to parameterize the collision efficiency E. The collision efficiency is governed by Brownian diffusion (in favour of small particles), inertial collision (for heavy particles) and interception (for large particles). The Brownian diffusion justifies that scavenging may be large for small particles (with diameters less than 0.01 μm) while the inertial effect justifies that scavenging may be large for coarse particles (with diameters bigger than 2 μm). The aerosols in the *Greenfield Gap* or *scavenging gap* (with diameters typically in the range [0.01; 2] μm) are more weakly scavenged. Notice that this gap is not always observed due to neglected effects (see below).

The application of the Buckingham π theorem gives E as a function of five dimensionless parameters: the raindrop Reynolds number ($Re = D_r U_{\text{drop}}/2\nu_{\text{air}}$), the particle Schmidt number ($Sc = \nu_{\text{air}}/D_B$ with $D_B = kTC_c/3\pi\mu_{\text{air}}d_p$ the particle Brownian diffusivity coefficient in $\text{m}^2\,\text{s}^{-1}$ and k the Boltzmann constant in $\text{J}\,\text{K}^{-1}$), the particle Stokes number ($St = 2u_{\text{grav}}/g \times (U_{\text{drop}} - u_{\text{grav}})/D_r$) and the ratio of diameters ($\phi = d_p/D_r$) and viscosities ($\omega = \mu_{\text{water}}/\mu_{\text{air}}$).

E is then computed by

$$E = \underbrace{\frac{4}{Re\,Sc}(1 + 0.4\,Re^{1/2}\,Sc^{1/3} + 0.16\,Re^{1/2}\,Sc^{1/2})}_{\text{Brownian diffusion}} + \underbrace{4\phi(\omega^{-1} + [1 + 2\,Re^{1/2}]\phi)}_{\text{interception}} + \underbrace{((St - S^*)/(St - S^* + 2/3))^{3/2}(\rho_p/\rho_{\text{water}})^{1/2}}_{\text{impaction}}, \tag{19}$$

with the critical Schmidt number $S^* = \frac{1.2 + 1/12\ln(1+Re)}{1+\ln(1+Re)}$. The three terms correspond to Brownian diffusion, interception and impaction, respectively. $E(D_r, d_p)$ and the different contributions are illustrated in Fig. 6 for a raindrop diameter $D_r = 0.1$ mm.

The collision efficiency is a function of both the raindrop diameter and the aerosol diameter (Fig. 7). The spread in the results with respect to the raindrop diameter has to be compared with the uncertainties in the representative diameter (Fig. 4).

3.2.3.4. Impact of a polydisperse distribution of aerosols. Mircea et al. (2000) take into account the polydisperse nature of aerosols and raindrops. The aerosol distribution is given by a lognormal law. This results in an affine parameterization for Λ

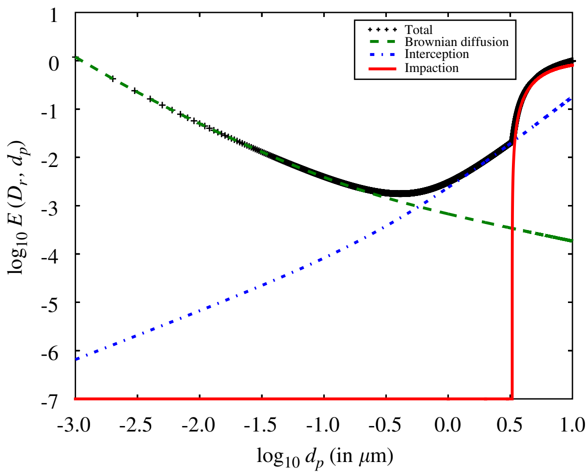

Fig. 6. Contributions of Brownian diffusion, interception and impaction for $E(D_r, d_p)$. The representative diameter for raindrops is $D_r = 0.1$ mm.

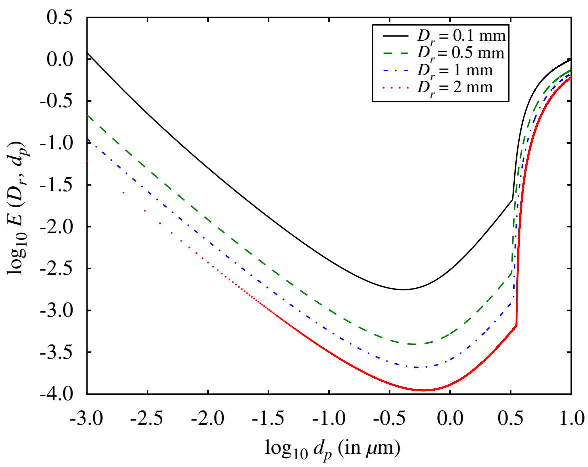

Fig. 7. Distribution of $E(D_r, d_p)$ with respect to d_p for representative diameters $D_r = 0.1$, 0.5, 1 and 2 mm.

as a function of rain intensity, $\Lambda = a + bp_0$. (a, b) are given as function of the aerosol type (rural, urban, marine): $a \in [1.58 \times 10^{-2} - 1.98]$ and $b \in [2.17 \times 10^{-3} - 3.19 \times 10^{-1}]$. The scavenging in an urban environment is much greater (one order of magnitude) than the scavenging in a remote environment (the maximal values correspond to the urban aerosol, the minimal values to the maritime aerosol). The main conclusion is also that the scavenging of a polydisperse distribution of aerosols is much greater than the scavenging of a monodisperse distribution (one order of magnitude at least). Moreover, there is a weak sensitivity with respect to the raindrop distribution.

We also refer to Zhao and Zheng (2006) for the investigation of appropriate numerical methods applied to the scavenging of polydisperse distributions (both for raindrops and aerosols, with lognormal distributions in the case study). Such methods are based on Monte Carlo techniques.

3.3. Parameterized models

3.3.1. Justification of the parameterization $\Lambda = Ap_0^B$

For a monodisperse aerosol distribution with a representative raindrop diameter D_r, $\Lambda = 1.5Ep_0/D_r$. As p_0 is usually in $\mathrm{mm\,h^{-1}}$, one has to apply a conversion factor $10^{-3}/3600$. With the spread in the estimation of D_r, Eq. (9), one gets

$$\Lambda \simeq [0.43 - 1.71] \times 10^{-3} E p_0^{[0.75-0.842]}. \tag{20}$$

For $E \in [0.1 - 1]$, this leads to

$$\Lambda \simeq [4.3 \times 10^{-5} - 1.71 \times 10^{-3}] p_0^{[0.75-0.842]}. \tag{21}$$

In Mircea and Stefan (1998), it is proven that the scavenging coefficient (integrated over the raindrop distribution) can be put under the form $\Lambda = Ap_0^B$. The assumptions are a Γ function for the raindrop distribution and a constant collision efficiency. B is a function of the parameters of the Γ distribution and of the raindrop falling velocity (supposed to be under the form $U_{\mathrm{drop}}(D_r) \propto D_r^{\alpha}$).

From Table 4, this leads to

$$\Lambda \simeq \begin{cases} [0.753 - 0.875] E p_0^{[0.78-0.86]} & \text{for strong rains,} \\ [1.91 - 1.95] E p_0^{[0.78-0.86]} & \text{for moderate rains,} \\ [20.56 - 26.67] E p_0^{[0.78-0.86]} & \text{for weak rains.} \end{cases} \tag{22}$$

Here, Λ is in $\mathrm{h^{-1}}$ and E (collision efficiency) has a constant value. With $E \simeq 0.1$ and after a conversion to $\mathrm{s^{-1}}$, one gets $\Lambda \simeq 2.3 \times 10^{-5} p_0^{0.8}$ for heavy rains and $\Lambda \simeq 6.6 \times 10^{-4} p_0^{0.8}$ for weak rains.

A similar approach is used in Andronache (2003) in order to justify the parameterization $\Lambda = Ap_0^B$ with a Marshall–Palmer distribution of raindrops intensity and a polydisperse aerosol distribution (Tables 7 and 8).

3.3.2. Empirical models derived from measurements

3.3.2.1. Measurements after the Chernobyl accident. Jylhä (1991) reports radar measurements in southern Finland after the Chernobyl accident. For cesium and iodine, this leads to $\Lambda \simeq [10^{-5} - 10^{-3}] p_0^{[0.5-0.7]}$ with an average value $10^{-4} p_0^{0.64}$ (Table 9). Notice that the rain intensity was weak (less than $1\,\mathrm{mm\,h^{-1}}$).

3.3.2.2. Measurements of ultrafine particles. Laakso et al. (2003) report results of measurements for 6 years over forests in southern Finland. Five-hundred and eighty-eight hours of rain have been measured with rain intensities ranging up to $20\,\mathrm{mm\,h^{-1}}$ with an average value of $0.9\,\mathrm{mm\,h^{-1}}$.

The scavenging coefficient has a minimal value for a diameter of $0.2\,\mu\mathrm{m}$. Scavenging coefficients range from 7×10^{-6} to 4×10^{-5} and have greater values than theoretically expected. A parameterized model is proposed for ultrafine particles ([10–510] nm) for rain intensities in the range $[0-20]\,\mathrm{mm\,h^{-1}}$

$$\log \Lambda(d_p, p_0) = a + \frac{b}{\log d_p^4} + \frac{c}{\log d_p^3} + \frac{d}{\log d_p^2} + \frac{e}{\log d_p} + 0.24\sqrt{p_0}. \tag{23}$$

Up to first-order, $\Lambda \sim \exp(0.24\sqrt{p_0})$.

One also refers to Andronache et al. (2006) for a model evaluation.

3.3.3. Parameterizations $\Lambda = A p_0^B$

We have already justified the parameterization $\Lambda = A p_0^B$. A typical value of B is 0.8. We have reported in Table 10 of some values collected in the literature.

Table 7
Fitting of polydisperse raindrop and aerosol distributions (Andronache, 2003)

A	B	Reference	Aerosol type
6.67×10^{-5}	0.7	Andronache (2003)	Urban
1.28×10^{-4}	0.7	id.	Remote continental
1.39×10^{-4}	0.7	id.	Marine
1.28×10^{-4}	0.7	id.	Rural
1.89×10^{-4}	0.7	id.	Free troposphere
9.44×10^{-5}	0.7	id.	Polar
2.44×10^{-4}	0.7	id.	Desert
2.22×10^{-4}	0.7	id.	Marine
8.33×10^{-5}	0.7	id.	Marine
1.94×10^{-4}	0.7	id.	Dust
1.00×10^{-4}	[0.67–0.76]	id.	Exp. data
3.50×10^{-4}	0.78	id.	In-cloud

Coarse fraction of the aerosol distribution (diameter above $10\,\mu\mathrm{m}$).

Table 8
Fitting of polydisperse raindrop and aerosol distributions (Andronache, 2003)

A	B	Reference	Aerosol type
2.34×10^{-7}	0.59	Sparmacher et al. (1993)	Exp. ($d_p = 0.23$)
3.14×10^{-7}	0.60	id.	Exp. ($d_p = 0.46$)
2.56×10^{-7}	0.94	id.	Exp. ($d_p = 0.98$)
1.72×10^{-6}	0.61	id.	Exp. ($d_p = 2.16$)
6.90×10^{-6}	0.92	Julya (1999)	Exp. (radionuclides)
$[2.36 \times 10^{-7} - 1.4 \times 10^{-6}]$	[0.59–0.61]	Andronache (2003)	Marine
$[2.78 \times 10^{-8} - 3.89 \times 10^{-8}]$	0.59	id.	Marine
2.36×10^{-7}	0.59	id.	Mountains

Submicronic fraction of the aerosol distribution. "Exp." stands for "experimental data".

Table 9
Parameterizations by fitting to observational data (Jylhä, 1991) after the Chernobyl accident

Species	A	B
^{131}I(p)	$7 \pm 5 \times 10^{-5}$	0.69 ± 0.12
^{133}I(p)	$1.6 \pm 3 \times 10^{-5}$	0.5 ± 0.2
^{134}Cs(p)	$2.8 \pm 0.6 \times 10^{-5}$	0.51 ± 0.07
^{137}Cs(p)	$3.4 \pm 0.9 \times 10^{-5}$	0.59 ± 0.08

Belot et al. (1988) advocate $A = 4 \times 10^{-5}$ and $B = 0.6$ for gaseous iodine. These values have been validated by other measurements (Caput et al., 1993) with an average value $A \simeq 8.2 \times 10^{-5}$.

For particulate iodine, the values are generally given on the basis of experimental data due to the underestimation provided by the theoretical values (related to the electrical interactions between liquid droplets and aerosols that are usually neglected).

CEC (1994) advocates the following values:

- for reactive iodine (probably "elemental"): $A \simeq 10^{-4}$;
- for organic iodine: $A \simeq 10^{-6}$;
- for submicronic particles ($r_p < 1$): $A \simeq 5 \times 10^{-5}$;
- for particles $r_p = 5$: $A \simeq 10^{-4}$;
- for coarse particles $r_p = 10$: $A \simeq 5 \times 10^{-4}$.

The parameterization of the NAME model (Maryon et al., 1992) takes into account the different types of scavenging (Table 11). For rainout, dynamic rain and convective rains are splitted (which is usually the case in the outputs of meteorological models). The increase in the scavenging coefficient for convective rain is also taken into account by other parameterizations (see Loosmore and Cederwall, 2004 and below).

A model based on measurement with a more complicated form is proposed in Baklanov and Sorensen (2001), with a focus on fine particles:

$$A(p_0, r_p) = \begin{cases} 8.4 \times 10^{-5} p_0^{0.79} & \text{if } r_p < 1.4\,\mu\text{m}, \\ g(r_p) f(p_0) & \text{if } 1.4 < r_p < 10\,\mu\text{m}, \\ f(p_0) & \text{if } r_p > 10\,\mu\text{m}, \end{cases} \tag{24}$$

with $f(p_0) \simeq 2.7 \times 10^{-4} p_0 - 3.62 \times 10^{-6} p_0^2$ and $g(r_p) \simeq -0.15 + 0.32 \quad r_p - 3.0 \times 10^{-2} r_p^2 + 9.34 \times 10^{-4} r_p^3$. A specific point is that it takes into account scavenging for the smallest particles (as opposed to Näslund and Holmström, 1993). The results obtained with this parameterization are given in Fig. 8. Notice that the general behaviour is different from the classical one and that there is no Greenfield gap.

For in-cloud scavenging, ENVIRON (2005) uses $A = 4.2 \times 10^{-4} p_0^{0.79}$ and is derived on basis similar to those used for the particles (see above) with a collision efficiency $E \simeq 0.9$ and a raindrop diameter given by a law similar to the first case in Table 5 ($D_r = 0.9 \times 10^{-4} p_0^{0.21}$ in mm Scott, 1978).

3.3.4. Other parameterizations

3.3.4.1. Parameterization based on the relative humidity. Brandt et al. (2002), following Pudykiewicz (1989), advocate a parameterization based on the relative humidity (RH). The advantages are that the rain intensity is usually highly uncertain and that it may describe in-cloud scavenging (which has the greatest impact for submicronic particles). When

Table 10
Some values of (A, B) for the parameterizations $\Lambda = A p_0^B$

Reference	Default	Particulate	Elem. iodine	Org. iodine
Raes et al. (1991)	$(5 \times 10^{-5};\ 0.8)$	—	—	—
Päsler-Sauer (2003)	—	$(8 \times 10^{-5};\ 0.8)$	$(8 \times 10^{-5};\ 0.6)$	$(8 \times 10^{-7};\ 0.6)$
Belot et al. (1988) and Caput et al. (1993)	8.2×10^{-5} (gas)	$(4 \times 10^{-5};\ 1)$ if $r_p < 1$ $(1.3 \times 10^{-4};\ 1)$ if $r_p > 1$	$(4 \times 10^{-5};\ 0.6)$	— —
CEC (1994)	—	5×10^{-5} if $r_p < 1$ 10^{-4} if $r_p = 5$ 5×10^{-4} if $r_p = 10$	10^{-4}	10^{-6}

For constant parameterizations, there is only one value. r_p is in μm.

Table 11
Parameterizations of the NAME model for rainout/washout (Maryon et al., 1992)

Scavenging	A	B
Washout	8.4×10^{-5}	0.79
Convective rainout	3.35×10^{-4}	0.79
Dynamic rainout	8.4×10^{-5}	0.79

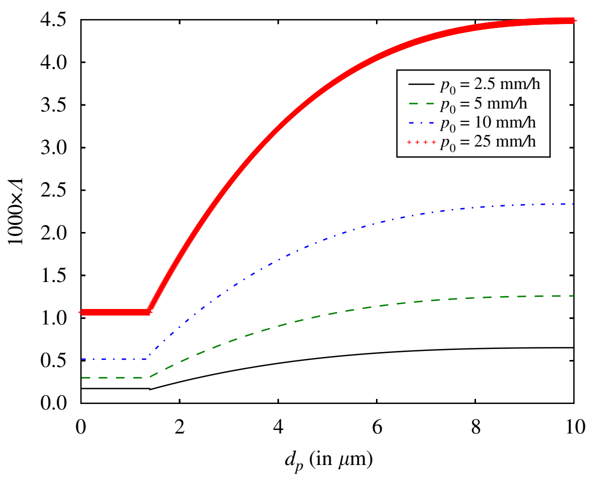

Fig. 8. Parameterizations of Baklanov and Sorensen (2001). Λ is multiplied by 1000.

RH is above a threshold $\mathrm{RH_t}$,

$$\Lambda = A \frac{\mathrm{RH} - \mathrm{RH_t}}{\mathrm{RH_s} - \mathrm{RH_t}}, \tag{25}$$

with $A = 3.5 \times 10^{-5}$. In Brandt et al. (2002), $\mathrm{RH_t} = 80\%$ and $\mathrm{RH_s} = 100\%$.

3.3.4.2. Parameterization of electrical effects. Taking into account the electrical effects may increase the scavenging coefficient up to a factor of 10 (Tripathi and Harrison, 2001). An additional term for the collision efficiency is proposed in Andronache (2004):

$$E_{es} = \frac{16 K C_c Q_r q_p}{3\pi \mu_{air} U_{drop} D_r^2 d_p}, \tag{26}$$

with $K = 9 \times 10^9$ (in $\mathrm{N\,m^2\,C^{-2}}$), Q_r and q_p are the charges (in Coulomb, C) of a raindrop and of a particle, respectively. A parameterization with respect to the size is proposed

$$Q_r = a\alpha D_r^2, \quad q_p = a\alpha d_p^2, \tag{27}$$

with $a = 0.83 \times 10^{-6}$ and α a parameter that depends on the electrical environment (from the microphysical and meteorological states). The minimal value of α is 2, the average value is 7.

3.3.4.3. Parameterization of violent rains. Loosmore and Cederwall (2004) advocate a correction to the existing parameterizations in order to describe the increase of the particle scavenging during convective rains. A crucial issue for the current models is that they usually underestimate the scavenging for convective events (probably due to phoretic effects and electrical effects, see above). Another reason is that the rain data are usually averaged in space and time.

The proposed correction consists in considering an aerosol of radius in $[0.1 - 5]\,\mu$m as an aerosol of radius $5\,\mu$m once p_0 is above a cut-off value (for instance $25\,\mathrm{mm\,h^{-1}}$). This brute-force approach is justified by the uncertainties in the microphysical data.

For instance with the parameterization of Baklanov and Sorensen (2001) (Fig. 8), a particle of radius 1 μm has a scavenging coefficient multiplied by a factor 3.5 above the threshold ($\frac{3.71}{1.06}$). Notice that this is relevant with the difference between the coefficients Λ for the convective washout and rainout (Table 11, $3.36 \times 10^{-4}/8.4 \times 10^{-5} \simeq 4$).

3.3.4.4. Sub-grid parameterization of the rain rate. The values of the precipitation intensity are *mean* values over a grid box. As for violent rains, this implies that the "true values" can be underestimated. Some parameterizations (which is not specific for radionuclides) use a *local rain rate* applied to the rainy fraction of the grid box. For instance, the simplest form is to replace the parameterization Ap_0^B by $f \times A(p_0/f)^B$ with f the rainy fraction (Rotstayn and Lohmann, 2002). f may be estimated on the basis of the cloud cover (cc).

In Stohl et al. (2005), only p_0 is modified as p_0/f with $f = \max(0.05, cc \times F(p_0))$ and $F(p_0)$ a function of the dynamic and convective precipitations.

3.3.4.5. Parameterization of snowfall. The scavenging by snow is poorly known and the measured data are usually not related to radionuclides. The uncertainties are related to the large variety of types and shapes of solid hydrometeors. In many works, it is usually assumed that the scavenging coefficient is the same one as for rain. The experimental data are indeed highly scattered. For instance, in Jylhä (2000), Λ is estimated below 10^{-6} (for an application to the removal of sulphur emission in the vicinity of a power station), a weak value. In Sparmacher et al. (1993), the scavenging coefficients for snow are about five times larger than the washout coefficients for rain (Table 12). We refer to Sparmacher et al. (1993) for the discussion about the measurement uncertainties (due to thermophoresis and diffusiophoresis).

A commonly used parameterization is given in Table 13 (for instance Sofiev et al., 2006; Baklanov and Sorensen, 2001, following Maryon et al., 1992). The values have to be compared to those given in Table 11 for rain scavenging.

We can also refer to Rotstayn and Lohmann (2002) with a parameterization under the form

$$\Lambda = \frac{E\beta(T)F}{2\rho_{\text{snow}}}, \tag{28}$$

Table 12
Enhancement of the scavenging coefficient parameterized by $\Lambda = A \times p_0^B$ for snowfall (fits from measurements, Sparmacher et al., 1993)

Particle diameter (in μm)	Washout (rain)	Snow
$d_p = 2.3 \times 10^{-1}$	$2.34 \times 10^{-7} p_0^{0.59}$	—
$d_p = 4.6 \times 10^{-1}$	$3.14 \times 10^{-7} p_0^{0.60}$	$1.6 \times 10^{-6} p_0^{0.62}$
$d_p = 9.8 \times 10^{-1}$	$2.56 \times 10^{-7} p_0^{0.94}$	$8.1 \times 10^{-7} p_0^{0.89}$
$d_p = 1.66$	—	$3.49 \times 10^{-6} p_0^{1.09}$
$d_p = 2.16$	$1.72 \times 10^{-6} p_0^{0.61}$	

Table 13
Parameterizations of the NAME model for the scavenging by snow (Maryon et al., 1992)

Scavenging	A	B
Below-cloud	8.05×10^{-5}	0.305
In-cloud (convective)	3.35×10^{-4}	0.79
In-cloud (dynamic)	8.05×10^{-5}	0.305

with E a collision efficiency for snow, ρ_{snow} the density for snow (typically $100\,\text{kg}\,\text{m}^{-3}$) and F a flux of precipitation (in $\text{kg}\,\text{m}^{-2}\,\text{s}^{-1}$). β is the slope coefficient of a Marshall–Palmer distribution for snow, given as a decreasing function of temperature (Rotstayn, 1997). The collision efficiency is supposed to be much lower than for rain, which lowers Λ (while the large density of snow leads to an increase).

3.3.4.6. Washout ratio. Another possible description of the washout is provided by the so-called washout ratio

$$W = \frac{C_{\text{aq}}}{C_{\text{g}}}, \tag{29}$$

with C_{aq} the dissolved concentration (with respect to water mass) and C_{g} the gaseous concentration (with respect to air mass). Chamberlain (1991) gives the following values for iodine (p. 131) and cesium (p. 92): $W_I \simeq 30$, $W_{Cs} \simeq 500$.

For gaseous iodine (cesium is bound on particles), one can try to link Λ and W. For the scavenging of a gas, the dissolved concentration at ground can be computed as in Seinfeld and Pandis (1998, p. 1005), p. 1005, Eq. (20)

$$(C_{\text{aq}})_{\text{a}} \simeq \frac{6K_{\text{c}}h}{U_{\text{drop}}D_{\text{r}}} C_{\text{g}}, \tag{30}$$

where K_c is the mass transfer coefficient and h the cloud height. U_{drop} (raindrop falling velocity) and D_r (representative diameter for the raindrops) have already been defined. Moreover, $(C_{\mathrm{aq}})_a = (\rho_{\mathrm{water}}/\rho_{\mathrm{air}})C_{\mathrm{aq}}$.

One has moreover

$$\Lambda = \frac{6 \times 10^{-3} p_0 K_c}{3600 U_{\mathrm{drop}} D_r}, \tag{31}$$

with p_0 in $\mathrm{mm\,h^{-1}}$. As $\rho_{\mathrm{water}}/\rho_{\mathrm{air}} \simeq 10^3$, one gets

$$\Lambda \simeq \frac{W p_0}{3600 h}. \tag{32}$$

This formula is also given in a similar form in Underwood (2001, p. 43). For $h \simeq 1000\,\mathrm{m}$ and $W_I \simeq 30$, one gets $\Lambda \simeq 10^{-5} p_0$. The magnitude is coherent with the previous parameterizations.

Notice that the washout ratio of organic iodine is low, which justifies the weak scavenging (Table 10).

4. Conclusion

We have reviewed the detailed and parameterized models of dry deposition and wet scavenging that can be used for radionuclides. A model hierarchy is available for the modellers, ranging from constant values (for instance for dry deposition velocities) to detailed microphysical modelling. Detailed models for particles are strongly related to the size distribution, which is usually poorly known even for the release.

For below-cloud scavenging, the parameterization of the scavenging coefficient $\Lambda = A p_0^B$ can be justified. The main uncertainties are actually related to the rain intensity. A key point is that there is a strong coherence among all available parameterizations.

There are at least two complementary ways for improving the modelling of these processes.

At the microphysical level, many effects have still to be included. For instance, electrostatic and phoretic effects may strongly impact the submicronic distribution and may explain the underestimation of the scavenging coefficient. Specific orographic effects related to atmospheric dispersion (orographic enhancement of the wet deposition through the "seeder-feeder" effect, Fournier et al., 2005) have also to be included in comprehensive models. The description of a polydisperse distribution of aerosols may also strongly modify the current parameterizations, usually based on a monodisperse distribution. The hygroscopic characteristics of particles may also impact these properties and are related to the chemical composition of particles to which radionuclides are bound (Chate et al., 2003). Notice that a key point is to have an aerosol model in which the radionuclides can be included.

A second approach is related to the meteorological fields and the way they are used. Using averaged quantities for rain intensities may underestimate the scavenging due to the underlying nonlinearities. Convective rains play a key role and are usually not well taken into account. Using data assimilation of measured data related to rain in dispersion models may be a challenging but promising task for improving the modelling.

Due to the large amount of uncertainties, one conclusion is that using ensemble forecast on the basis of a set of different parameterizations and of different meteorological data is required for modelling the dispersion of radionuclides (Galmarini et al., 2004; Mallet and Sportisse, 2006).

Acknowledgements

I thank my colleagues Yelva Roustan and Denis Quélo from CEREA for fruitful discussions. Thanks to Monika Krysta for her careful lecture. This work has been led in the framework of a joint project with the French Institute for Nuclear Safety (IRSN, Olivier Isnard) devoted to the modelling of the atmospheric dispersion of radionuclides.

I also thank the anonymous reviewers for their remarks.

References

Andronache, C., 2003. Estimated variability of below-cloud aerosol removal by rainfall for observed aerosol size distribution. Atmospheric Chemistry and Physics 3, 131–143.

Andronache, C., 2004. Diffusion and electric charge contributions to below-cloud wet removal of atmospheric ultre-fine aerosol particles. Aerosol Science and Technology 35, 1467–1482.

Andronache, C., Grönholm, T., Laakso, L., Phillips, V., Venäläinen, A., 2006. Scavenging of ultrafine particles by rainfall at a boreal site: observations and model estimations. Atmospheric Chemistry and Physics 6, 4739–4754.

Baklanov, A., 1999. Parameterisation of the deposition processes and radioactive decay: a review and some preliminary results with the DERMA model. Technical Report 99-4, DMI, 1999.

Baklanov, B., Sorensen, J.H., 2001. Parameterisation of radionuclides deposition in atmospheric long-range transport modelling. Physics and Chemistry of the Earth B 26 (10), 787–799.

Belot, Y., Caput, C., Guenot, J., 1988. Etude bibliographique du lavage par la pluie des radionucléides particulaires et gazeux émis en situation accidentelle. Technical report, IRSN et EDF.

Brandt, J., Christensen, J.H., Frohn, L., 2002. Modelling transport and deposition or caesium and iodine from the Chernobyl accident using the DREAM model. Atmospheric Chemistry and Physics 2, 397–417.

Budyka, A.K., 2000. Phase transformation of iodine and other volatile radionuclides in free atmosphere. Journal of Aerosol Science 31 (S1), 480.

Caput, C., Camus, H., Gauthier, D., Belot, Y., 1993. Etude expérimentale du lavage de l'iode par la pluie. Radioprotection 28 (1), 15–22.

CEC, 1994. Probabilistic accident consequence uncertainty analysis. Dispersion and deposition uncertainty assessment. Technical Report EUR 15855 EN, CEC.

Chamberlain, A.C., 1991. Radioactive Aerosols. Cambridge University Press, Cambridge.

Chate, D.M., Rao, P.S.P., Naik, M.S., Momin, G.A., Safai, P.D., Ali, K., 2003. Scavenging of aerosols and their chemical species by rain. Atmospheric Environment 37, 2477–2484.

Clark, M.J., Smith, F.B., 1988. Wet and dry deposition of Chernobyl releases. Nature 332 (17), 245.

ENVIRON, 2005. User's Guide CAMx—Version 4.20. Technical report, ENVIRON International Corporation.

Fournier, N., Weston, K.J., Dore, A.J., Sutton, M.A., 2005. Modelling the wet deposition of reduced nitrogen over the British Isles using a Lagrangian multi-layer atmospheric transport model. Quarterly Journal of the Royal Meterological Society 131, 703–722.

Gallagher, M., Fontan, J., Wyers, P., Ruijgrok, W., Duyzer, J., Hummelsjoj, P., Pilegaard, K., Fowler, D., 1999. Biosphere–Atmosphere exchange of pollutants and trace substances, Atmospheric Particles and their Interactions with Natural Surfaces, Springer, Berlin, 1999.

Galmarini, S., Bianconi, R., Klug, W., Mikkelsen, T., Addis, R., Andronopoulos, S., Astrup, P., Baklanov, A., Bartniki, J., Bartzis, J.C., et al., 2004. Ensemble dispersion forecasting—part I: concept, approach and indicators. Atmospheric Environment 38 (28), 4607–4617.

Garland, J.A., 2001. On the size dependence of particle deposition. Water, Air, and Soil Pollution: Focus 1, 323–332.

Greenfield, S., 1957. Rain scavenging of radioactive particulate matter from the atmosphere. Journal of Meteorology 14, 115–125.

Haas, H., Memmesheimer, M., Geiss, H., Jacobs, H.J., Laube, M., Ebel, A., 1990. Simulation of the Chernobyl radioactive cloud over Europe using the EURAD model. Atmospheric Environment 24A (3), 673–692.

Hanna, S.R., Gifford, F.A., Yamartino, R.J., 1991. Long-range radioactive plume transport simulation model/code. Phase I. Technical report, USNRC Division of Contracts and Property Management, 1991.

Henzing, J.S., Olivié, D.J.L., van Velthoven, P.F.J., 2006. A parameterization of size resolved below cloud scavenging of aerosols by rains. Atmospheric Chemistry and Physics 6, 3363–3375.

Jylhä, K., 1991. Empirical scavenging coefficients of radioactive substances released from Chernobyl. Atmospheric Environment 25A (2), 262–270.

Jylhä, K., 2000. The scavenging of air pollutants by precipitation and its estimation with the aid of weather radar. Ph.D. Thesis, University of Helsinki, Finland, Report 50.

Julya, K., 1999. Relationship between the scavenging coefficient for pollutants in precipitation and the radar reflectivity factor. Part I: derivation. Journal of Applied Meteorology, 1421–1434.

Klug, W., Graziani, G., Gripa, G., Pierce, D., Tassone, C., 1992. Evaluation of long range atmospheric transport models using environmental radioactivity data from the Chernobyl accident: the ATMES report. Technical report, Elsevier Applied Science, 1992.

Laakso, L., Grönholm, T., Rannik, U., Kosmale, M., Fiedler, V., Vehkamäri, H., Kulmala, M., 2003. Ultrafine particle scavenging coefficients calculated from 6 years field measurements. Atmospheric Environment 37, 3605–3613.

Loosmore, G.A., Cederwall, R.T., 2004. Precipitation scavenging of atmospheric aerosols for emergency response applications: testing an updated model with new real-time data. Atmospheric Environment 38, 993–1003.

Mallet, V., Sportisse, B., 2006. Ensemble-based air quality forecasts: a multi-model approach applied to ozone. Journal of Geophysical Research 111 (D18), 18302.

Maryon, R.H., Smith, F.B., Conwy, B.J., Goddard, D.M., 1992. The UK nuclear accident response model (NAME). Progress in Nuclear Energy 26 (2), 85–104.

Mircea, M., Stefan, S., 1998. A theoretical study of the microphysical parameterization of the scavenging coefficient as a function of precipitation type and rate. Atmospheric Environment 32 (17), 2931–2938.

Mircea, M., Stefan, S., Fuzzi, S., 2000. Precipitation scavenging coefficient: influence of measured aerosol and raindrop size distribution. Atmospheric Environment 34, 5169–5174.

Müller, H., Pröhl, G., 1993. A dynamic model for assessing radiological consequences of nuclear accidents. Health Physics 64 (3), 232–252.

Näslund, E., Holmström, H., 1993. Inclusion of a three-dimensional washout coefficient in ADPIC. Technical Report UCRL-ID-114054, Lawrence Livermore National Laboratory, 1993.

Näslund, E., Thaning, L., 1991. On the settling velocity in a nonstationary atmosphere. Aerosol Science and Technology 14, 247–256.

Ogorodnikov, B.I., Budyka, A.K., Skitovitch, V.I., 1994. Radioactive aerosols near Chernobyl in 1986–1992. Journal of Aerosol Science 25, S269–S270.

Päsler-Sauer, J., 2003. Description of the atmospheric dispersion model ATSTEP. Version RODOS PV 5.0. Technical Report RODOS(RA2)-TN(03)-01, Forschungszentrum Karlsruhe GMBH.

Pöllänen, R., Valkama, I., Toivonen, H., 1997. Transport of radioactive particles from the Chernobyl accident. Atmospheric Environment 31 (21), 3575–3590.

Pruppacher, H.R., Klett, J.D., 1998. Microphysics of Clouds and Precipitation. Kluwer Academic Publishers, Dordrecht.

Pryor, S.C., Barthelemie, R.J., Geernaert, L.L.S., Ellermann, T., Perry, K.D., 1999. Speciated particle dry deposition to the sea surface: results from ASEPS'97. Atmospheric Environment 33, 2045–2058.

Pudykiewicz, J., 1989. Simulation of the Chernobyl dispersion with a 3D hemispheric tracer model. Tellus 41B, 391–412.

Quélo, D., Krysta, M., Bocquet, M., Isnard, O., Minier, Y., Sportisse, B., 2006. Validation of the POLYPHEMUS system: the ETEX, Chernobyl and Algeciras cases. Atmospheric Environment, in revision.

Raes, F., Tassone, C., Grippa, G., Zarimpas, N., Graziani, G., 1991. Updating long-range transport model predictions using real-time monitoring data in case of nuclear accidents with release to the atmosphere. Atmospheric Environment 25A (12), 2807–2814.

Roselle, S.J., Binkowski, F.S., 1999. Chapter 11: cloud dynamics and chemistry. Science algorithms of the EPA Models-3. Technical Report 600/R-99/030, EPA.

Rotstayn, L., 1997. A physically based scheme for the treatment of stratiform clouds and precipitation in large-scale models. I—Description and evaluation of the microphysical processes. Quarterly Journal of the Royal Meteorological Society 123, 1227–1282.

Rotstayn, L.D., Lohmann, U., 2002. Simulation of the tropospheric sulfur cycle in a global model with a physically based cloud scheme. Journal of Geophysical Research 107 (D21), 4592.

Scott, B.C., 1978. Parameterization of sulfate removal by precipitation. Journal of Applied Meteorology 17, 1375–1389.

Sehmel, G.A., 1980. Particle and gas deposition: a review. Atmospheric Environment 14, 983–1011.

Seinfeld, J.H., 1985. Atmospheric Physics and Chemistry of Air Pollution. Wiley, New York.

Seinfeld, J.H., Pandis, S.N., 1998. Atmospheric Chemistry and Physics. Wiley-interscience, New York.

Slinn, S.A., Slinne, W.G.N., 1980. Prediction for particle deposition on natural waters. Atmospheric Environment 14, 1013–1016.

Sofiev, M., Siljamo, P., Valkama, I., Ilvonen, M., Kukkonen, J., 2006. A dispersion modelling system SILAM and its evaluation against ETEX data. Atmospheric Environment 40, 674–685.

Sparmacher, H., Fülber, K., Bonka, H., 1993. Below-cloud scavenging of aerosol particles: particle-bound radionuclides. Experimental. Atmospheric Environment 27A (4), 605–618.

Sportisse, B., Djouad, R., 2003. Mathematical investigation of mass transfer for atmospheric pollutants into a fixed droplet with aqueous chemistry. Journal of Geophysical Research 108 (D2), 4073.

Sportisse, B., Du Bois, L., 2002. Numerical and theoretical investigation of a simplified model for the parameterization of below-cloud scavenging by falling raindrops. Atmospheric Environment 36, 5719–5727.

Stohl, A., Forster, C., Frank, A., Seibert, P., Wotawa, G., 2005. Technical note: the Lagrangian particle dispersion model FLEXPART version 6.2. Atmospheric Chemistry and Physics 5, 2461–2474.

Thykier-Nielsen, S., Deme, S., Mikkelsen, T., 1999. Description of the atmospheric dispersion module RIMPUFF. Technical Report RODOS(WG2)-TN(98)-02, Forschungszentrum Karlsruhe GMBH, 1999.

Tost, H., Jöckel, P., Kerkweg, A., Sander, R., Lelieveld, J., 2006. Technical note: a new comprehensive SCAVenging submodel for global atmospheric chemistry modelling. Atmospheric Chemistry and Physics 6, 565–574.

Travnikov, O., Ilyin, I., 2005. Regional model MSCE-HM of heavy metal transboundary air pollution in Europe. Technical Report 6/2005, EMEP/MSC-E.

Tripathi, S.N., Harrison, R.G., 2001. Scavenging of electrified radioactive aerosols. Atmospheric Environment 35, 5817–5821.

Underwood, B., 2001. Review of deposition velocity and washout coefficient. Technical report, AEA Technology, Harwell, 2001.

Venkatram, A., Pleim, J., 1999. The electrical analogy does not apply to modelling dry deposition of particles. Atmospheric Environment 33, 3075–3076.

Wesely, M.L., 1989. Parameterization of surface resistance to gaseous-dry deposition in regional scale numerical models. Atmospheric Environment 23, 1293–1304.

Wesely, M.L., Hicks, B.B., 2000. A review of the current status of knowledge on dry deposition. Atmospheric Environment 34, 2261–2282.

de Wolf, D.A., 2001. On the Laws–Parsons distribution of raindrop sizes. Radio Science 36, 639–642.

Zhao, H., Zheng, C., 2006. Monte Carlo solution of wet removal of aerosols by precipitation. Atmospheric Environment 40, 1510–1525.

Zhang, L., Gong, S., Padro, J., Barrie, L., 2001. A size-segregated particle dry deposition scheme for an atmospheric aerosol module. Atmospheric Environment, 549–560.